Critical-Point Structure in Finite Nuclei

A. Leviatan

Racah Institute of Physics, The Hebrew University, Jerusalem 91904, Israel

Abstract. Properties of quantum shape-phase transitions in finite nuclei are considered in the framework of the interacting boson model. Special emphasis is paid to the dynamics at the critical-point of a general first-order phase transition.

Keywords: Quantum shape-phase transitions, critical-points, interacting boson model of nuclei
PACS: 21.60Fw, 21.10Re, 05.70.Fh

Phase transitions associated with a change of shape are known to occur in dynamical systems such as nuclei. Recently, it has been recognized that such quantum shape-phase transitions are amenable to analytic descriptions at the critical points [1, 2]. For nuclei these analytic benchmarks of criticality were obtained in the geometric framework of a Bohr Hamiltonian for macroscopic quadrupole shapes. In particular, the E(5) [1] (X(5) [2]) benchmark is applicable to a second- (first-) order shape-phase transition between spherical and deformed γ-unstable (axially-symmetric) nuclei. Empirical evidence of these benchmarks have been presented [3, 4]. An important issue concerning phase transitions in real nuclei is the role of a finite number of nucleons. This aspect can be addressed in the algebraic framework of the interacting boson model (IBM) [5] which describes low-lying quadrupole collective states in nuclei in terms of a system of N monopole (s) and quadrupole (d) bosons representing valence nucleon pairs. The three dynamical symmetry limits of the model: U(5), SU(3), and O(6), describe the dynamics of stable nuclear shapes: spherical, axially-deformed, and γ-unstable deformed. A geometric visualization of the model is obtained by an intrinsic energy surface defined by the expectation value of the Hamiltonian in the coherent (intrinsic) state [6, 7]

$$|\beta,\gamma;N\rangle \;=\; (N!)^{-1/2}(b_c^\dagger)^N|0\rangle\,, \tag{1}$$

where $b_c^\dagger=(1+\beta^2)^{-1/2}[\beta\cos\gamma d_0^\dagger+\beta\sin\gamma(d_2^\dagger+d_{-2}^\dagger)/\sqrt{2}+s^\dagger]$. For the general IBM Hamiltonian with one- and two-body interactions, the energy surface takes the form

$$E(\beta,\gamma) \;=\; N(N-1)(1+\beta^2)^{-2}\left[a\beta^2-b\beta^3\cos3\gamma+c\beta^4\right]\,. \tag{2}$$

The coefficients a,b,c involve particular linear combinations of the Hamiltonian's parameters [8, 9]. The quadrupole shape parameters in the intrinsic state characterize the associated equilibrium shape. Phase transitions for finite N can be studied by an IBM Hamiltonian involving terms from different dynamical symmetry chains [6]. The nature of the phase transition is governed by the topology of the corresponding energy surface. In a second-order phase transition, the energy surface is γ-independent and has a single minimum which changes continuously from a spherical to a deformed γ-unstable phase. At the critical point, $a=b=0$, and the energy-surface acquires a flat behaviour ($\sim\beta^4$)

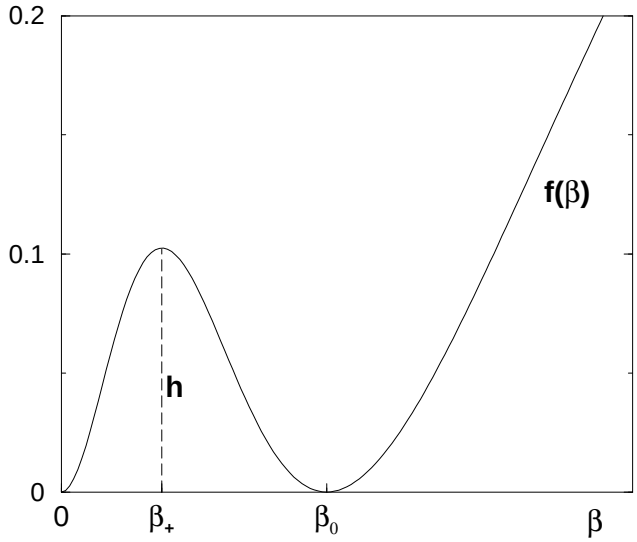

FIGURE 1. The IBM energy surface, Eq. (3), at the critical point of a first-order phase transition. The position and height of the barrier are $\beta_+ = \frac{-1+\sqrt{1+\beta_0^2}}{\beta_0}$ and $h = f(\beta_+) = \frac{1}{4}\left(-1+\sqrt{1+\beta_0^2}\right)^2$ respectively.

for small β. This is the situation encountered in the U(5)-O(6) phase transition. In a first-order phase transition the energy surface has two coexisting minima which become degenerate at the critical point. The U(5)-SU(3) phase transition is a special case of this class, for which the barrier separating the spherical and axially-deformed minima is extremely small, and hence the critical energy surface is rather flat. Numerical [3, 10] and (approximate) analytic [11, 12] studies within the IBM, show that the U(5)-O(6) [U(5)-SU(3)] critical Hamiltonians capture the essential features of the E(5) [X(5)] models which employ infinite square-well potentials. In the present contribution we consider the properties of a general first-order phase transition with an arbitrary barrier. In this case the critical energy surface satisfies $b > 0$ and $b^2 = 4ac$, and for $\gamma = 0$ has the form

$$\begin{aligned} E_{cri}(\beta) &= cN(N-1)f(\beta) \\ f(\beta) &= \beta^2(1+\beta^2)^{-2}(\beta-\beta_0)^2 \, . \end{aligned} \tag{3}$$

As shown in Fig. 1, $E_{cri}(\beta)$ exhibits degenerate spherical and deformed minima, at $\beta = 0$ and $\beta = \beta_0 = \frac{2a}{b} > 0$. The value of β_0 determines the position $(\beta = \beta_+)$ and height (h) of the barrier separating the two minima in a manner given in the caption. To construct an Hamiltonian with such an energy surface, it is advantageous to resolve the critical Hamiltonian into intrinsic and collective parts [8, 9]

$$H = H_{int} + H_c \, . \tag{4}$$

The intrinsic part of the Hamiltonian (H_{int}) is defined to have the equilibrium condensate $|\beta = \beta_0, \gamma = 0; N\rangle$ as an exact zero-energy eigenstate and to have an energy surface as in Eq. (3). It can be transcribed in the form

$$H_{int} = h_2 P_2^\dagger \cdot \tilde{P}_2 \, , \tag{5}$$

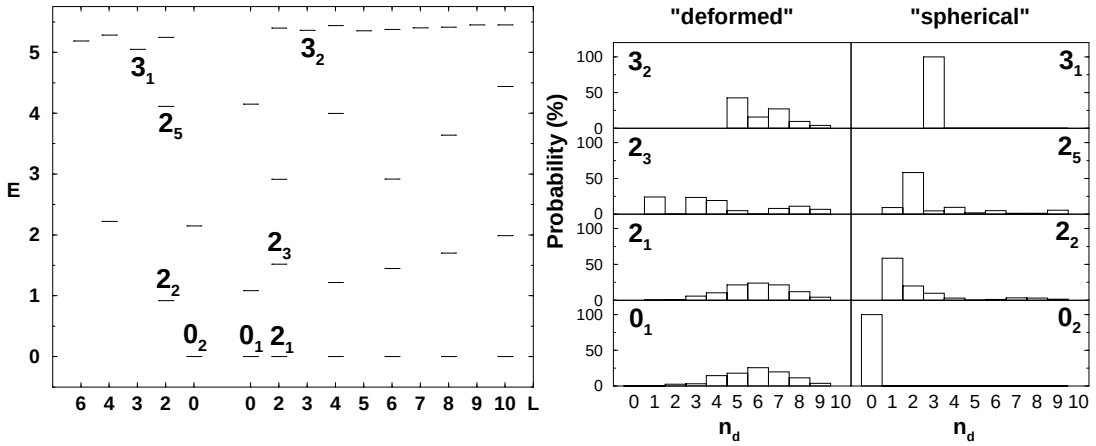

FIGURE 2. Left potion: spectrum of H_{int}, Eq. (5), with $h_2 = 0.1$, $\beta_0 = 1.3$ and $N = 10$. Right portion: the number of d bosons (n_d) probability distribution for selected eigenstates of H_{int}.

with $P^\dagger_{2,\mu} = \beta_0 s^\dagger d^\dagger_\mu + \sqrt{\frac{7}{2}}\left(d^\dagger d^\dagger\right)^{(2)}_\mu$. By construction H_{int} has a set of solvable deformed eigenstates with energy $E = 0$, which are the states $|\beta = \beta_0; N, L\rangle$ with angular momentum $L = 0, 2, 4, \ldots, 2N$ projected from the intrinsic state $|\beta = \beta_0, \gamma = 0; N\rangle$. It has also solvable spherical eigenstates: $|N, n_d = \tau = L = 0\rangle \equiv |s^N\rangle$ and $|N, n_d = \tau = 3, L = 3\rangle$ with energy $E = 0$ and $E = 3h_2\left[\beta_0^2(N-3)+5\right]$ respectively. For large N the spectrum of H_{int} is harmonic, involving 5-dimensional quadrupole vibrations about the spherical minimum with frequency ε, and both β and γ vibrations about the deformed minimum, with frequencies ε_β and ε_γ given by

$$\varepsilon = \varepsilon_\beta = h_2 \beta_0^2 N \quad , \quad \varepsilon_\gamma = \frac{9}{1+\beta_0^2}\,\varepsilon_\beta \ . \tag{6}$$

For the acceptable range $0 \le \beta_0 \le 1.4$, the γ-band is expected to be considerably higher than the β-band. All these features are present in the exact spectrum of H_{int} shown in Fig. 2, which displays a zero-energy deformed ($K = 0$) ground band, degenerate with a spherical $(n_d = 0)$ ground state. The remaining states are either predominantly spherical, or deformed states arranged in several excited $K = 0$ bands below the γ band. The coexistence of spherical and deformed states is evident in the right portion of Fig. 2, which shows the n_d decomposition of wave functions of selected eigenstates of H_{int}. The "deformed" states show a broad n_d distribution typical of a deformed rotor structure. The "spherical" states show the characteristic dominance of single n_d components that one would expect for a spherical vibrator. In particular, as mentioned above, the solvable $L = 0^+_2$ and $L = 3^+_1$ states are pure $U(5)$ states.

The collective part (H_c) of the full Hamiltonian, Eq. (4), is composed of kinetic terms which do not affect the shape of the energy surface. It can be transcribed in the form

$$H_c \;=\; c_3\left[\hat{C}_{O(3)} - 6\hat{n}_d\right] + c_5\left[\hat{C}_{O(5)} - 4\hat{n}_d\right] + c_6\left[\hat{C}_{\overline{O(6)}} - 5\hat{N}\right] \ , \tag{7}$$

where $\hat{n}_d$ and $\hat{N} = \hat{n}_d + \hat{n}_s$ are the d-boson and total-boson number operators respectively. Here $\hat{C}_G$ denotes the quadratic Casimir operator of the group G as defined in [9]. In

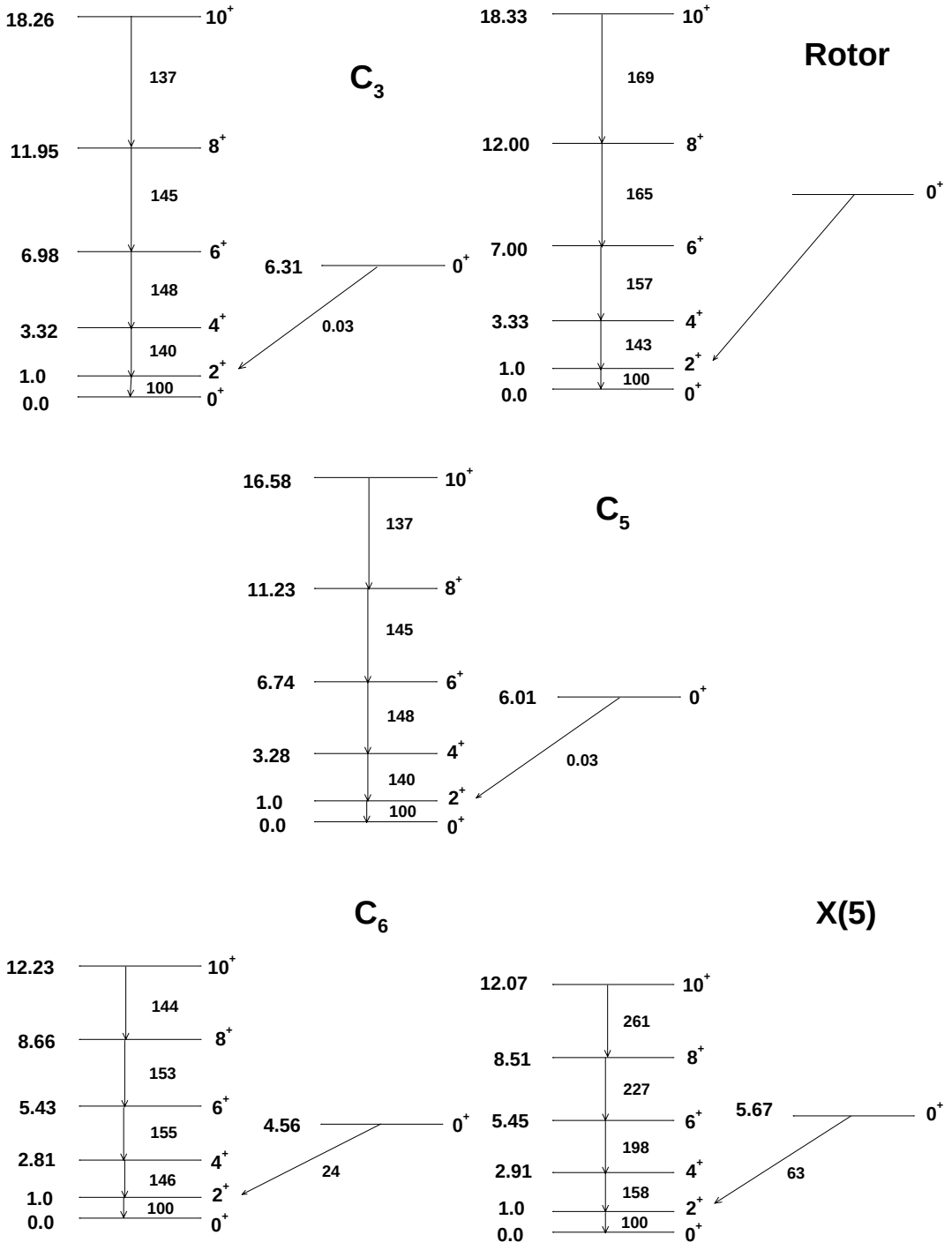

FIGURE 3. The spectrum of the critical Hamiltonian $H = H_{int} + H_c$, Eqs. (5) and (7), with $\beta_0 = 1.3$, $N = 10$, and $c_3/h_2 = 0.05$ or $c_5/h_2 = 0.1$ or $c_6/h_2 = 0.05$. The spectrum of a rigid rotor and the X(5) model is shown for comparison. Energies are in units of the first excited state, $E(2_1^+) - E(0_1^+) = 100$, and $B(E2)$ values are in units of $B(E2; 2_1^+ \to 0_1^+) = 100$.

general H_c splits and mixes the states of H_{int}. Fig. 3 shows the effect of different rotational terms in H_c, with parameters indicated in the caption. For the high-barrier case considered here, ($\beta_0 = 1.3, h = 0.1$), the calculated spectrum resembles a rigid-rotor ($E \sim a_N L(L+1)$) for the c_3-term, a rotor with centrifugal stretching ($E \sim a_N L(L+1) - b_N[L(L+1)]^2$) for the c_5-term, and a X(5)-like spectrum for the c_6-term. In all cases the B(E2) values are close to the rigid-rotor Alaga values. This behaviour is different from that encountered when the barrier is low, *e.g.*, for the U(5)-SU(3) critical Hamiltonian with $\beta_0 = 1/2\sqrt{2}$ and $h \approx 10^{-3}$, where both the spectrum and E2 transitions are similar to the X(5) predictions. Considerable insight of the underlying structure at the critical point is gained by examining the 2×2 mixing matrix between the spherical ($|s^N\rangle$) and deformed ($\beta; N, L = 0\rangle$) states. The derived eigenvalues serve as eigenpotentials, and the corresponding eigenvectors are identified with the ground- and first-excited $L = 0$ states. The deformed states $|\beta; N, L\rangle$ with $L > 0$ are identified with excited members of the ground-band with energies given by the L-projected energy surface $E_L^{(N)} = \langle \beta; N, L | H_{int} + H_c | \beta; N, L \rangle$, which can be evaluated in closed form

$$\begin{aligned} E_L^{(N)}(\beta) &= h_2 (\beta - \beta_0)^2 \Sigma_{2,L}^{(N)} + c_3 \left[L(L+1) - 6 D_{1,L}^{(N)} \right] + c_5 \left[-\beta^4 S_{2,L}^{(N)} + D_{2,L}^{(N)} \right] \\ &\quad + c_6 \left[-(1+\beta^2)^2 S_{2,L}^{(N)} + N(N-1) \right] . \end{aligned} \tag{8}$$

Here $\Sigma_{2,L}^{(N)}$, $D_{1,L}^{(N)}$, $D_{2,L}^{(N)}$ and $S_{2,L}^{(N)}$ denote the expectation values of $\hat{n}_s \hat{n}_d$, $\hat{n}_d$, $\hat{n}_d(\hat{n}_d - 1)$ and $\hat{n}_s(\hat{n}_s - 1)$ respectively in $|\beta; N, L\rangle$. The value of β in the indicated wave functions and energies, is chosen at the global minimum of the lowest eigenpotential. This procedure yields an excellent approximation to the structure of yrast states at the critical point, which is then used to derive accurate finite-N estimates to the corresponding energies and E2 rates [13]. The same prescription is applicable also to a first-order phase transition with a low-barrier [12]. For a second-order critical point, the determination of the effective β-deformation involves an $O(5)$ projection without two-level mixing [11].

This work was supported by the Israel Science Foundation.

REFERENCES

1. F. Iachello, *Phys. Rev. Lett.*,**85**, 3580 (2000).
2. F. Iachello, *Phys. Rev. Lett.*, **87**, 052502 (2001).
3. R. F. Casten and N.V. Zamfir, *Phys. Rev. Lett.*, **85**, 3584 (2000).
4. R. F. Casten and N. V. Zamfir, *Phys. Rev. Lett.*, **87**, 052503 (2001).
5. F. Iachello and A. Arima, *The Interacting Boson Model*, Cambridge Univ. Press, Cambridge 1987.
6. A. E. L. Dieperink, O. Scholten and F. Iachello, *Phys. Rev. Lett.*, **44**, 1747 (1980).
7. J. N. Ginocchio and M. W. Kirson, *Phys. Rev. Lett.*, **44**, 1744 (1980).
8. M. W. Kirson and A. Leviatan, *Phys. Rev. Lett.*, **55**, 2846 (1985).
9. A. Leviatan, *Ann. Phys. (NY)*, **179**, 201 (1987).
10. F. Iachello and N. V. Zamfir, *Phys. Rev. Lett.*, **92**, 212501 (2004).
11. A. Leviatan and J. N. Ginocchio, *Phys. Rev. Lett.*, **90**, 212501 (2003).
12. A. Leviatan, *Phys. Rev. C*, **72**, 031305 (2005).
13. A. Leviatan, (2005), in preparation.